A Spring-block Model for Barkhausen Noise

K. Kovács[1], Y. Brechet[2] and Z. Néda[1,3]
[1] *Babeş-Bolyai University, Dept. of Physics, str. Kogălniceanu 1, RO-400084 Cluj-Napoca, Romania*
[2] *Institut National Polytecnique de Grenoble, ENSEEG-LTPCM, 38402 Saint Martin d'Heres, France*
[3] *Centro de Fisica do Porto, 4099-002 Porto, Portugal*
E-mail: zneda@phys.ubbcluj.ro

A simple mechanical spring-block model is introduced for studying magnetization phenomena and in particular the Barkhausen noise. The model captures and reproduces the accepted microscopic picture of domain wall movement and pinning. Computer simulations suggest that the model is able to reproduce the main characteristics of hysteresis loops and Barkhausen jumps. The statistics of the obtained Barkhausen jumps follows several scaling laws, in qualitative agreement with experimental results. The simplicity and the invoked mechanical analogies make the model attractive for computer simulations and pedagogical purposes.

PACS numbers:75.60.Ej, 75.60.-d, 05.10.-a

I. INTRODUCTION

Barkhausen noise (BN) belongs to the family of the so-called crackling noises [1]. It appears as a series of discrete and abrupt jumps in the magnetization whenever a ferromagnetic sample is placed under varying external magnetic field. In standard ferromagnets where magnetization is driven by the motion of domain walls, it is believed that the BN is a consequence of the fast movement of domain walls between pinning centers, which are either defects or impurities. The present paper introduces a simple and successful mechanical analogy for describing this classic magnetization phenomenon. We do not intend to make a complete description for a particular experiment or material, there are several specific and successful models in this aspect (for a recent review see [2]). Our stated aim is to introduce a very general and simple model which is attractive for computer simulation studies and captures the minimum ingredients necessary to model BN.

The Barkhausen phenomenon is interesting from several points of view. From a practical side, by measuring the BN there is a possibility for non-destructive and non-invasive material testing and control. On the other hand, from a pure conceptual viewpoint, by studying the BN one might reach a better understanding of the complex dynamics of domain walls during magnetization processes in the presence of pinning centers opposing to the motion of magnetic walls. It is also a clear example for the dynamics of a system presenting collective pinning when a quenched disorder is present.

Since its discovery (1917) BN has been intensively studied [2]. Numerous measurements were done to clarify the statistical properties of the BN [3–5]. Regarding the nature of the Barkhausen noise (white noise, $1/f$ noise, or $1/f^2$ noise) a variety of conflicting statements can be found in the experimental literature. The most extensive measurements and data analysis were performed by Spasojevic et al. [3] with a commercial VITROVAC 6025-X metal glass (quasi 2D) sample. After performing the statistical and numerical calculations, they have found: (i) power-law type distribution for signal duration with scaling exponent -2.22, (ii) power-law behavior for signal area with scaling exponent -1.77, and (iii) power-law type power spectrum with scaling exponent -1.6 to -1.7. From here they concluded that BN is not pure $1/f$, nor $1/f^2$ (Brownian) type noise, but something between these two. Plewka, et al. [4] performed measurements (and calculations) with a similar experimental setup on an amorphous ribbon in an open magnetic circuit. They obtained instead a value around -0.9 for the scaling exponent of the power spectrum. From this result they concluded that BN is typically $1/f$ noise. O'Brien and Weissman [5] performed measurements with a SQUID magnetometer on an amorphous iron-based metallic alloy (2605TCA) and they suggested that BN is much closer to a white noise than a $1/f$ noise and differs sharply from most typical $1/f$ noises.

BN received a special attention in the context of self-organized criticality. Self -organized criticality (SOC) is a term used for a class of complex phenomena where non-equilibrium broadband noise in driven systems reflects a type of self-organization, producing states with power-law correlations closely analogous to critical phenomena [6]. Some of the ingredients of SOC were known to be potentially relevant to BN. In some cases, magnetization changes have been directly observed to occur via avalanche process in the domain topology [7]. These avalanches exhibit some scaling effects, at least over a narrow range of parameters, and their behavior has been described by a SOC model [8,9]. There are however other approaches that put under doubt the relevance of the SOC concept to BN. O'Brien and Weissman [5] for example argued that the presumed $1/f$ nature of BN and the observed power-law distributions are not necessarily evidences of SOC, but rather the consequences of the scaling properties of quenched disorder in the material.

Many conceptually different models were elaborated to explain BN and its scaling properties. Without the intention of making a complete review, here we will mention only a few selected theoretical approaches. Alessandro et al. [10] proposed a single degree of freedom model (ABBM model) that considers the motion of a single domain wall in a spatially rough coercive field created by the defects. They concluded that a mean-field approximation is adequate, and found power-law behavior for the Barkhausen pulse size distribution. Another model [16] which is strongly related to the previous one considers the motion of a single flexible domain wall in an uncorrelated disordered medium. This approach leads to a power-law distribution of the avalanche sizes (exponent -1.5) and durations (exponent -2), and yields an exponent -2 for the scaling of the power spectrum. Travesset et al. [11] and Perkovic et al. [12] described the BN in terms of avalanches near a critical point. They used the zero-temperature random field Ising model (RFIM), in which the effect of the pinning centers was taken into account as a normally distributed local random field. This model was able to account for the power-laws characteristic for the distribution of avalanche sizes, signal area and signal duration. Another theoretical attempt by O. Narayan [13] considers a multiple degrees of freedom model, studying the relaxation dynamics of a single domain wall in a two-dimensional Ising system. This model yields a power-law with critical exponent -1.5 for the power spectrum. The model predicts that in other dimensions different critical exponents are expected, for example in one-dimension the critical exponent for the power spectrum should be zero. This result is in contradiction with the prediction of the mean-field approximation for the single degree of freedom model [10], which predicts the value -2 for the exponent, independently of the dimensionality of the model. Urbach, Madison and Markert considered a model (known as the UMM model) [14] where three relevant forces for the interface dynamics are taken into account, namely the interface elastic energy, a random quenched disorder and external driving. However, in the UMM model the pinning force is accounted in an unrealistic manner. Pinning is considered simply as an additive stochastic term in the value of the total force. The motion of the interface is governed simply by the sum of the three forces, and the main signature of pinning as a static friction which has the property to oppose a net force with a given strength, is lost. The UMM model has the advantage that it can be studied in arbitrary dimension and leads power-law distribution for the Barkhausen avalanche sizes. The obtained exponents for the Barkhausen signal area distribution is in reasonable agreement with the experimental results.

Despite the numerous complex and conceptually different approaches the Barkhausen phenomenon is still an open and much debated problem [15]. The spring-block model introduced in this paper offers an over-simplified but elegant alternative, which can be successfully used for pedagogical purposes. As it is shown in the following, this model has the potential to qualitatively explain the general signatures and scaling laws characteristic to BN, with parameters which can be at least qualitatively related to micro-structural features (wall density, pinning centers strength and density).

II. THE SPRING-BLOCK MODEL

The model is essentially a one-dimensional spring-block system. It is aimed to reproduce the accepted microscopic picture of domain wall dynamics for 180 degree Bloch-walls which separate inversely oriented $(+|-|+|-|+\dots)$ magnetic domains (Fig.1).

We assume that the domain walls are pinned by defects and impurities, and cannot move unless the resultant force acting on them is bigger than the strength of the F_p pinning force. When the resulting force is greater than the pinning force, the wall simply jumps in the resulting force direction on the next pinning center. Apart of this pinning force there are two other types of forces acting on each domain wall. To understand these forces let us consider the i-th wall (which separates the $(i-1)$-th and i-th domain) free to move and all other walls fixed. One of the forces acting on the domain wall, F_H , results from the magnetic energy of the domains i and $(i-1)$ in an external magnetic field. Let us consider the external magnetic field as sketched in Fig.1. The interaction energy between one magnetic domain and the external magnetic field:

$$W = -c_H \cdot H \cdot M \qquad (1)$$

where c_H is a constant, H is the strength of the external magnetic field and M is the magnetization of the domain (the positive direction both for M and H is taken upward). Taking into account that the $(i-1)$ and i neighboring domains are oppositely oriented, their total energy of interaction with the external magnetic field is:

$$W(i) = W_{i-1} + W_i = -c_H \cdot H \cdot \Delta M \qquad (2)$$

The quantity ΔM (the sum of magnetizations of the neighboring $(i-1)$ and i domains) is related to the two domains' length's difference ($\Delta x = x_i - x_{i-1}$) as

$$\Delta M = (-1)^i \gamma \cdot \Delta x \qquad (3)$$

where γ is constant relating the size of the domain with its magnetization. From (2) and (3) it results:

$$W(i) = (-1)^{i+1} \cdot c_H \gamma \cdot H \cdot \Delta x \qquad (4)$$

The force F_H acting on domain wall i can be determined considering the δL elementary work performed by this force, when the wall is displaced by a distance dl

$$\delta L = F_H \cdot dl = -dW(i) = (-1)^i c_H \gamma \cdot H \cdot d(\Delta x) = \\ = (-1)^i c_H \gamma \cdot H \cdot 2dl \qquad (5)$$

$$F_H = \frac{\delta L}{dl} = (-1)^i 2c_H\gamma \cdot H = (-1)^i\beta \cdot H \tag{6}$$

with $\beta = 2c_H\gamma$ another constant. In our model for the sake of simplicity we define the units such that $\beta = 1$. For positive values of the external magnetic field this force encourages the increase of the domains oriented in the + direction, and for negative values of the external magnetic field this force tends to increase the size of the domains oriented in the $-$ direction.

A second type of force, F_m, acting on both sides of the domain walls, is due to the magnetic self-energy of each domain. This force tends to minimize the length of each domain. It can be immediately shown that F_m is proportional with the length of the considered domain. The E_i magnetic self-energy of a magnetic domain i has the form

$$E_i = c_m {M_i}^2 \tag{7}$$

where c_m is a constant. As in the previous case

$$dE_i = c_m \cdot d({M_i}^2) = -\delta L = -F_m dl \tag{8}$$

and from here the F_m force:

$$F_m = -\frac{dE_i}{dl} = -2c_m(M_i)\frac{dM_i}{dl} \approx -2c_m\gamma^2 \cdot x_i \frac{dx_i}{dl} = = -2c_m\gamma^2 x_i = -f_m x_i \tag{9}$$

The constant f_m is an important coupling parameter in this model and acts as the elastic constant of a mechanical spring.

The system of the F_p, F_m and F_H forces can be now easily mapped on a mechanical spring-block model.

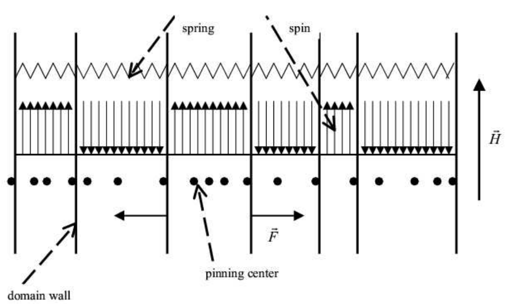

FIG. 1. Sketch of the mechanical spring-block model

The main constituents in this mechanical model are randomly distributed pinning centers, rigid walls sitting on pinning centers (describing Bloch-walls) separating + and $-$ oriented domains and springs between the walls (describing the F_m forces). The strength of the pinning centers (pinning forces), F_p, are randomly distributed following a normal distribution. Walls can be only on pinning centers and two walls are not allowed to occupy the same pinning center. This constraint implies that the number of magnetic domains and domain walls are kept constant and are thus a-priori fixed. Domains cannot totally disappear and new domains cannot appear during magnetization phenomena. The elastic springs are ideal with zero equilibrium length and with the tension linearly proportional with their length. The tension in the elastic springs will reproduce the F_m forces. Beside the pinning forces and the tensions in the springs there is an extra force acting on each wall. The strength of this force is proportional with the exterior magnetic field's intensity, it is the same for all walls but its direction is inverse for $+|-$ and $-|+$ walls. This force will reproduce the F_H forces.

It has to be noticed that in the absence of applied field and pinning centers the walls at equilibrium will be equally spaced. Since we impose the number of walls to be constant, this means that the average wall spacing will be given by the classical expression corresponding to the minimization of the magnetostatic energy and of the total wall energy.

The model as it stands is grossly simplified: in a real system the walls are 2D, they have an anisotropic stiffness, so they may be described by the dynamics of their trace (1D) on the plane perpendicular to the easy magnetization axis. The depinning of this line is unlikely to occur as a whole, but it will probably propagate all along the line. Because of all these simplifications the present model cannot be expected to be directly connected to microstructural features (such as the density and strengths of the physical pinning centers), neither to be quantitative. The present model is important mainly for conceptual purposes, to define the minimum ingredients necessary to capture the various power laws observed. In addition, the relative importance of the pinning potential (via F_p the strength and N_p the number of pinning centers) and of the coupling between walls (via F_m) can be qualitatively investigated.

The dynamics of this model is aimed to reproduce real magnetization phenomena. First N_p pinning centers are randomly distributed on a fixed length (L) interval, and their strengths are assigned. Than a fixed N_w number of walls are randomly spread over the pinning centers ($N_w \ll N_p$) and connected by ideal springs. Neighboring domains are assigned opposite magnetic orientation. The external F_H force is first chosen zero (corresponding to $H = 0$), and we let the system relax to an equilibrium configuration. To achieve this we calculate the resultant of the F_m forces on each wall. If the strength of the pinning force acting on one wall is smaller than the force resulting from the tension of the springs attached to it, the wall will jump in the direction of the resultant force on the next pinning site. However, if this pinning site is already occupied, the wall remains in its original position. We assume that the time needed for the system to achieve equilibrium is zero. It is important to note that one event (jump) can trigger many other events leading to avalanche-like processes. The above dynamics is continued until the equilibrium is satisfied for each domain wall. The order in which the position of the walls is updated is random.

Once the initial equilibrium configuration is reached we begin to simulate the magnetization phenomenon. The value of the F_H external force is increased step-by-step (corresponding to an increasing H magnetic field intensity), and for each new F_H value an equilibrium position of the system is searched. In equilibrium the magnitude of the resulting force on each wall should be less than the pinning force acting on that wall. In each equilibrium configuration we calculate the total magnetization of the system as:

$$M = \sum_i l_i \cdot s_i \tag{10}$$

where l_i is the length of domain i, and s_i is it's orientation: $+1$ for positive orientation, and -1 for negative orientation. We increase F_H until no more walls can move and the magnetization reaches its maximal value. Starting from this we decrease step-by-step the value of F_H, and for each new value the equilibrium configuration is again reached and the total magnetization computed. The system is driven until oppositely oriented saturation. From here we increase again the value of F_H and many hysteresis cycles are simulated. Throughout the whole simulation we assume that the process of magnetization is performed at a rate slow enough so that at each step the system can reach a position of equilibrium in a sort of quasi-static magnetization process.

During the simulation we are monitoring the variation of the magnetization focusing on the shape of the hysteresis loop, jump size distribution, power spectrum, Barkhausen signal duration and signal area distribution functions.

The hysteresis loop is the history-dependent relation between the magnetization M and the external magnetic field H when the value of H is increased and decreased successively. The jump size distribution ($g(s)$) is the distribution function for the obtained values of abrupt jumps in M throughout many hysteresis loops. The Barkhausen signal is given by $\frac{dM}{dt}$ and it is proportional with an electric voltage that would be induced in a detecting electromagnetic coil. Under the assumption of a quasi-static process performed at a constant rate of increase of the applied magnetic field H, the derivatives with respect to time which enter the generation of Barkhausen noise are proportional to derivations with respect to H: $\frac{Dom}{dH}$. This means that the magnitude of the Barkhausen jumps is not to be understood as absolute values, but would depend on the rate of increase of H.

We determined the power spectrum ($P(f)$) of the obtained Barkhausen signal by using a Fast Fourier Transform (FFT). The situation we have considered here for modeling the power spectrum is highly idealized. Beside the implicit assumption that the external field is varied quasi-stationary and at constant rate, we have neglected the interaction between the physical phenomena responsible for the noise (unpinning avalanches) and the detection device. Thus, we emphasize that the power spectrum determined from this simulation should be viewed under these constraints.

We also study the shape of the histograms for Barkhausen signal duration distribution ($g(d)$) and signal area distribution $g(A)$. In terms of our simulation the signal duration measures the number of consecutive dH steps when Barkhausen jumps occur ($\Delta M/dH$ is nonzero). Signal area is also related to this quantity: it represents the area under $\Delta M/dH$ versus H for a nonzero $\Delta M/dH$ sequence.

The parameters of the model are: N_p – the number of pinning centers; N_w – the number of Bloch-walls ($N_w \ll N_p$); f_m – the coupling constant between the neighboring domain walls (corresponds to the elastic constant in the case of coupled springs); and the dH – driving rate of the external magnetic field (change in H for one simulation step). The total length of the magnetic domains is considered to be of unity ($L = 1$) and the distribution function for the strength of the pinning forces was considered to be normally distributed and has been fixed. We use rigid boundary conditions: the first Bloch-wall compulsory occupies the first pinning center, the last wall occupies the last pinning center, and these bounding walls cannot move. This constraint means that the geometrical size of our model system doesn't change during the simulation. As we already mentioned the number of Bloch-walls and magnetic domains are also fixed within this model, domains can shrink or grow, but they cannot appear or disappear during the simulation. This constraint is also a serious drawback of the model, since in real magnetization phenomena domains can disappear or appear, and thus the number of interfaces are not constant. This drawback is expected to be serious in the saturation limit, but not in the low magnetization region.

III. EFFECTS OF THE FREE PARAMETERS

Before presenting the simulation results let us discuss here the expected effects of the free parameters. We will use adimensional units for the forces, their strengths are determined relatively to the adimensional strength of the pinning forces. The f_m, β, H and x quantities are defined through equations (6) and (9) and they are also considered to be adimensional. The pinning forces can have only positive values and they are normally distributed on the [0,1] interval with mean $\langle F_p \rangle = 0.5$ and standard deviation $\sigma = 0.1$.

a. Influence of N_p. As N_p increases the pinning centers are closer to each other which causes many small Barkhausen jumps. Concurrently, small number of pinning centers result less but bigger jumps in magnetization. From the above arguments one can conclude that the value of the parameter N_p influences directly the shape of the hysteresis loops and the obtained jump size distribution histogram. As N_p increases the simulation is more and more time consuming, since many small jumps and thus many intermediate equilibrium positions are available. This is an important factor that limits the value of the used N_p parameter. We have performed our calculations with N_p between 1000 and 10000.

b. Influence of N_w. N_w determines the number of magnetic domains in our model system. Large values of N_w require long computation times since the equilibrium becomes more and more sophisticated. Because N_w should be much smaller than N_p, increasing N_w would lead also to large N_p values, which again makes the simulation technically difficult. In our simulations we considered $N_w = 200$. The parameter N_w determines also how strongly the springs are stressed. Small value of N_w means that the walls are far from each other and the coupling springs between them are strongly tensioned. In this case the obtained avalanches in wall movements are usually longer. The N_p/N_w ratio is one of the most relevant quantities regarding the outcome of the simulations. We consider the N_p/N_w ratio to be relatively "small" if it is less than 10 and "large" if it is greater then 30. For small N_p/N_w ratio springs are not very stressed, thus small number of jumps will occur during the magnetization process and strong external magnetic field is needed in order to make the walls jump. After relatively few jumps saturation is reached and the walls will form "pairs" that can be destroyed only by inverting the external magnetic field's direction. For large N_p/N_w ratio the existence of relatively many pinning centers causes many small jumps. The small number of Bloch-walls causes springs to be stretched and favors the occurrence of jumps even for weak external magnetic fields. A large number of steps is needed until saturation is reached and the walls are stopped by their neighbors. In simulations we varied this parameter between 10 and 50 and studied it's influence on the BN statistics.

c. Influence of f_m. Since this parameter acts in our spring-block model like the elastic constant of the springs, its value determines the value of attractive forces between neighboring walls. As f_m increases the coupling becomes stronger, and weak external magnetic field is enough to make the walls jump. For small f_m values the springs are weakly coupled, so a stronger external magnetic field is needed to make the walls jump. In our model the N_p/N_w ratio and the f_m parameters are strongly related to each other. In the case of many pinning centers and relatively small number of walls (equivalent with N_p/N_w large) even for weak coupling (f_m around 10) many jumps occur and equilibrium states are easily reached. When the N_p/N_w ratio is small (around 10) weak coupling requires strong external magnetic fields in order to make walls jump and only a relatively small number of jumps are possible. In this parameter region the hysteresis loops have only a very limited number of jumps and these jumps occur only for high H magnetic field values. If the coupling gets stronger (still N_p/N_w low) equilibrium states are very difficult to reach, walls jump back and forth and hysteresis loops are totally damaged. When the N_p/N_w ratio is large (around 30), this means that there are many pinning centers and relatively small number of walls. In this case weak coupling (f_m around 10) will be enough to make walls jump even for low H values because the springs are strongly stressed. The expected result is the existence of many small jumps along the whole hysteresis loop. For stronger couplings equilibrium is again difficult to reach and the hysteresis curves are expected to be damaged. It is obvious that finding the optimal parameter region for the simulation is crucial. Wrong parameters that generate damaged hysteresis loops, or situations where the equilibrium states are difficult to reach (walls jump back and forth many times consecutively) will cause significant artifacts in the jump-size, signal-duration or signal-area distribution functions.

e. Influence of the driving rate in H (dH). This parameter is also important for all the considered distribution functions. It is obvious that small dH (around 0.001) steps produce very many "short" and small jumps, while larger steps (dH between 0.01-0.005) make possible only the "longer" Barkhausen-signals. The latter means that larger dH steps leads usually to many consecutive jumps (i.e. large avalanches). Very small dH value will divide the bigger and longer jumps into many tinny jumps. In the experiments greater dH steps correspond to the case where the ferromagnetic sample is submitted to a relatively fast changing driving field, thus it reaches the saturation magnetization after few number of large jumps. In the experiments it is reported however [3,5,9,17] that they used very low frequencies (< 1 Hz) for the driving field. This is the reason why we have chosen to make the simulations with relatively small dH steps (0.001) that corresponds to quasi-stationary driving and allows the system to relax to a closer equilibrium configuration during each step of the magnetization – demagnetization process.

Pondering the effects of all the above described parameters, we have found that the best parameter region that produces simulation results in agreement with the experimental ones is the following: $N_p = 5000 - 10000$, $N_w = 100 - 200$ ($N_p/N_w = 50 - 100$), $f_m = 10$, $dH = 0.001$. The simulation results presented in this paper are all obtained for the parameter values: $N_p = 10000$, $N_w = 200$, $f_m = 10$, $dH = 0.001$. The relevant distribution functions were obtained by averaging on 100 independent configurations (different initial states for the walls and pinning centers). For illustrating that the obtained scaling exponents are not altered by finite-size effects (i.e. the exponents characteristic for the thermodynamic limit are reached) we also plot the characteristic curves obtained for $N_p = 5000$.

IV. SIMULATION RESULTS

Characteristic hysteresis loops are plotted on Fig. 2. The shape of the obtained hysteresis curves satisfies our expectations and fulfills all the requirements for real magnetization phenomena. On these curves one can detect many discrete jumps with different sizes, thus the model exhibits BN. In addition, when the sample is driven consecutively through many hysteresis cycles the magnetization curves do not follow exactly the same path, although the parameters of the simulation were unchanged. The qualitative shape of the hysteresis curve is quite stable for a wide range of the free parameters.

All the distribution functions we have computed for the statistics of the Barkhausen noise are normalized and defined as

$$g(y) = \frac{N(y, y + dy)}{N_t \cdot dy}, \tag{11}$$

where N_t denotes the total number of occurrences, $N(y, y + dy)$ is the number of occurrences with sizes between y and $y + dy$, y is the quantity under focus which can be jump size (s), signal duration (d) or signal area (A).

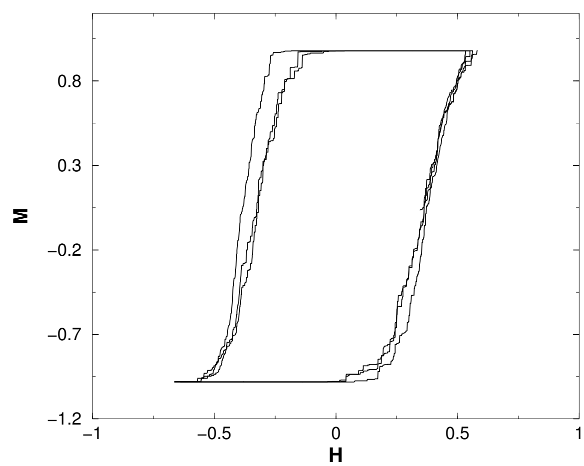

FIG. 2. Hysteresis loops obtained by simulation with parameter values: $N_p = 10000$, $N_w = 200$, $f_m = 10$ and $dH = 0.001$.

The jump size distribution histogram in our simulations corresponds to the avalanche size distributions from experiments and it is the most relevant distribution for the characterization of the Barkhausen noise. For N_p=10000 and 5000, $N_w = 200$, $f_m = 10$, $dH = 0.001$, the jump-size distribution function is plotted on Fig. 3.

Based on this graph we can conclude: (i) the jumps size distribution function shows power-law with exponential tail; the exponent of the power-function part is -0.7; (ii) there is a clear exponential cut-off which is the result of finite-size effect; (iii) the region where this scaling is valid extends over three decades in our simulation for $N_p = 10000$ and represents the trend that is to be followed if the system is increased to infinity. (iv) finite size effects do not influence any more the obtained -0.7 scaling exponent, since the results for $N_p = 5000$ indicates the same power-law. (v) as expected for smaller N_p values the scaling regime is shorter, and the exponential cutoff appears sooner.

The fact that our simulation results indicate a power-law distribution in the thermodynamic limit means that jump (avalanche) sizes exhibits a scale-invariance, a feature that is expected to be common for all types of crackling noises.

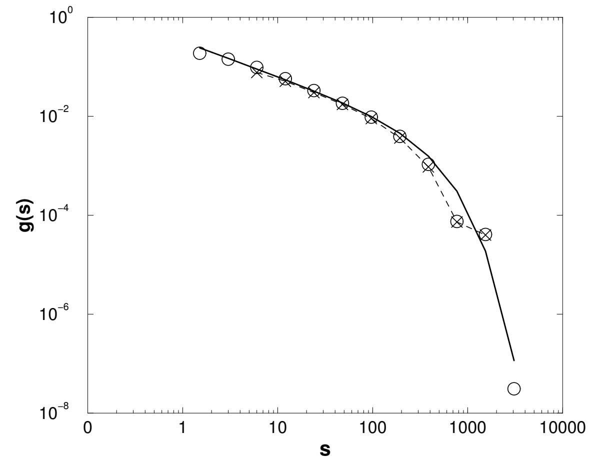

FIG. 3. Jump size distribution function for $N_p = 10000$ (circles) and $N_p = 5000$ (x symbols, dashed line) ($N_w = 200$, $f_m = 10$, $dH = 0.001$). The solid line indicates a fit to the simulation data $N_p = 10000$: power-function with exponential cut-off: $g(s) = 0.32 s^{-0.7} exp(-003s)$

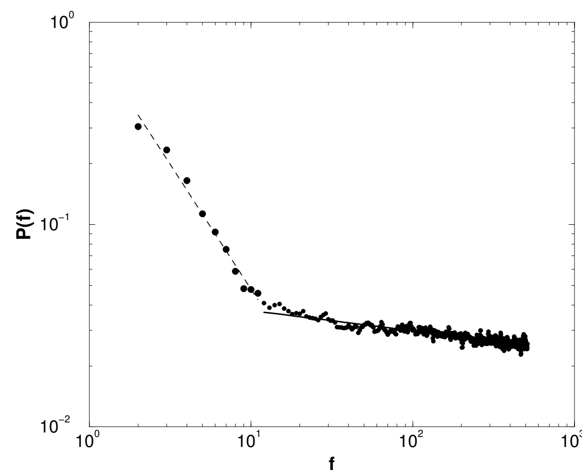

FIG. 4. Power spectrum of the simulated BN ($N_p = 10000$; $N_w = 200$; $f_m = 10$; $dH = 0.001$). Two regions with different behavior are clearly distinguishable: low-frequency region – power-law with slope $= -1.23$ (dashed line) and high-frequency region – almost white noise, the slope of the fitted power-function being -0.1 (solid line)

The power spectrum obtained from simulation indicates different noise-type in the low- and high-frequency region. For low frequencies the power spectrum is fitted well with a power-function with exponent -1.23, that indicates a $1/f$ type noise. In the high-frequency region the power spectrum suggests white noise over two decades, though there is a small measurable non-zero slope -0.1

(Fig. 4.).

We emphasize it again that this power spectrum has to be treated with care since we do not have real time in simulations, and thus we cannot define a proper frequency. Time evolution is substituted with the driving rate dH of the external field and it is considered that equilibrium is reached for each simulation step. We have plotted thus the "power spectrum" in terms of the $1/dH$ – type "frequency", assuming the unit time as the time needed to change the external magnetic field by dH.

On Fig. 5. we plotted the signal duration distribution function for $N_p = 10000$ and $N_p = 5000$. As it results from the graph in our simulations we have only two decades of data. The results are fitted with a power-law with exponential cut-off. The results suggest that for the obtained scaling exponent the thermodynamic limit is reached. From the results for $N_p = 10000$ we get the exponent of the power-function -1.33 and the exponent of the cut-off -0.045. The cut-off again is a finite-size effect as it is clear from the plotted results for $N_p = 10000$ and $N_p = 5000$. This approach is valid for $\frac{dH}{dt} = const.$

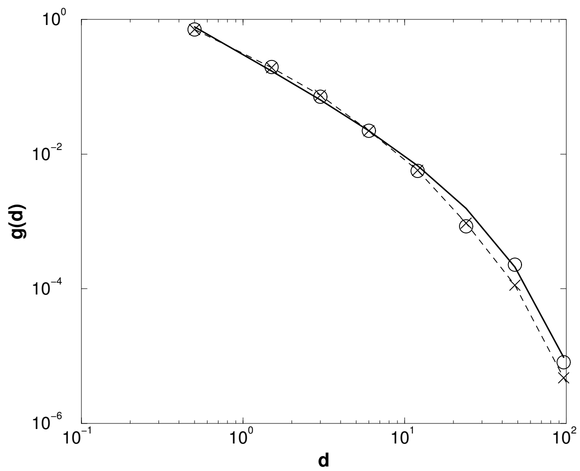

FIG. 5. Distribution function for signal duration for $N_p = 10000$ (circles) and $N_p = 5000$ (x symbols, dashed line), $N_w = 200$; $f_m = 10$; $dH = 0.001$. The solid line indicates the fit to simulation data with $N_p = 10000$, using a power-function with exponential cut-off: $g(d) = 0.31 d^{-1.33} exp(-0.045 d)$

On Fig. 6. we plotted the signal area distribution function, again for $N_p = 10000$ and $N_p = 5000$. The curves suggest a power-law behavior over four decades of data. The exponent of the fitting power-function is -1.66. As expected, the scaling is much nicer for bigger N_p values.

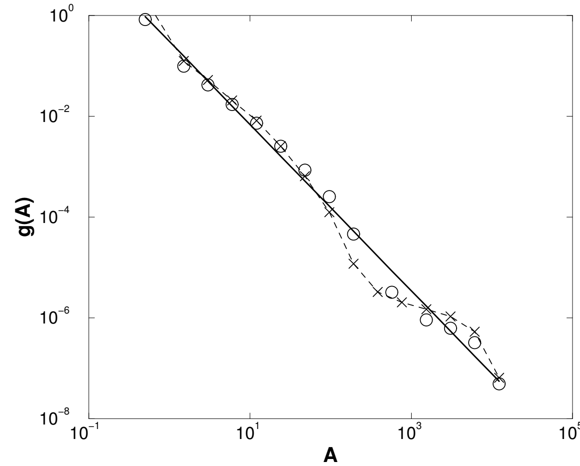

FIG. 6. Signal area distribution function for $N_p = 10000$ (circles) and $N_p = 5000$ (x symbols, dashed line), $N_w = 200$; $f_m = 10$; $dH = 0.001$. The solid line is a power-function fit to the $N_p = 10000$ simulation data with slope $= -1.66$.

V. DISCUSSION

Comparison of the obtained simulation results with the experimental ones yields the following conclusions:

1. The simulated hysteresis loops are qualitatively in good agreement with the ones obtained in experiments. On the simulated hysteresis loops one can observe many Barkhausen jumps with various sizes, just as it is expected from the experimental results. We can also learn from the graph that the hysteresis loops do not follow the same path when the system goes through several cycles. As an illustration, on Fig. 2 we presented three consecutive loops.

2. The shape of the simulated jump size distribution function predicts in the thermodynamic limit ($N_w \to \infty$, $N_p \to \infty$, $N_p/N_w \to \infty$) a tendency toward a power-law. Our results on relatively small systems suggest a power-law behavior with an exponent -0.7. Experimentally this quantity is usually not investigated, since it is difficult to detect those very small changes in the magnetization.

3. As already emphasized, we do not consider the power spectrum obtained within our model relevant. A first reason for this is that we do not have real time in our simulations and the equilibration of the system is instantaneously in real time. A second reason why we do not consider our results for the power-spectrum realistic is that the detection of the Barkhausen signal is without any inertia. An inertia of the detection device (which in experiments always appears) would definitely alter the nature of the results. Despite all these concerns, our result which suggests a white noise (exponent of the power spectrum ≈ 0) for high frequencies is in agreement with O. Narayan's [13] prediction for one-dimensional systems. For low frequencies however, our results suggest a $1/f$ type noise, and supports the experimental results of Spasojevic et al. ([3]) and Plewka et al. ([4]). In this sense

our results support most of the experimental data, and suggests, that the frequency region in which the power-spectrum is computed is important in deciding the type of the measured BN noise.

4. The experimental results for the signal duration and the signal area [3,9,14,17] distribution indicate a scaling behavior for both quantities.

For the signal duration distribution the experimentally measured exponents were -2.2 [3] and -1.64 to -2.1 [9]. Although the measured values are strongly dependent on the used material and experimental setup, all the experiments agree in the validity of the power-law distribution. Our simulations show a power-law with exponential cutoff, suggesting thus a scaling with an exponent -1.33, somehow smaller than those obtained in experiments. We have to remember however that one has to be careful when comparing our theoretical results for the signal durations and signal areas with the experimental ones. We have to remember that in our simulations the time is not a real one and the simulation time-step is governed by dH, which is taken as constant. It is also assumed that the system relaxes to equilibrium in each simulation step. Our simulation results would be appropriate thus for those experimental conditions where the H driving field is slowly and linearly changed in time. Many of the performed experiments might not satisfy these conditions. It is also known that the driving rate has an influence on the measured power-law exponents [18] in the limit of high frequencies. However in the limit of low frequencies, the results seem to be stable, and the experimental results cited by us are all in this limit.

For the signal area distribution experiments obtained power-laws with exponents ranging from -1.7 to -1.8 [3], -1.74 to -1.88 [9], -1.23 to -1.35 [17] and -1.33 [14]. As in the case of the signal duration distribution, the measured value is again strongly dependent on the used material and experimental setup. Our simulations predict a clear scaling on four orders of magnitude with an exponent -1.66, which is in reasonable agreement with the results of [3] and [9].

From all these scaling results we conclude that the power-law tendencies suggested in our simulations can explain at least qualitatively the measured statistics of the Barkhausen noise.

VI. CONCLUSIONS

The simple one-dimensional model presented in this paper is successful in qualitatively reproducing the measured statistics of the Barkhausen noise. The model captures the main elements of the microscopic dynamics for the phenomenon and in spite of its gross simplification, it contains all the necessary ingredients to describe the statistics of the BN. The model is also suitable for pedagogical purposes and can be easily implemented on computer.

Despite of the encouraging results the model is far from being perfect. One very important feature is the absence of the temperature as parameter. Also, there is no real time in simulations, and only the value of the dH magnetization step determines the rate at which time evolves in our simulations. The model doesn't account for the pinning mechanism and the strength of the pinning forces. It is an oversimplified one-dimensional approximation for the complex three-dimensional domain topology. Seemingly the most serious problem of the present model is that the number of domain walls is a priori fixed and domains cannot appear or disappear during the dynamics. There are many other complex and more specialized models, elaborated for different experimental setups and different materials ([2]). Our model cannot, and does not intend to compete with these ones in describing the experimental results. The stated aim of the introduced model is to give a simple and somehow general model for the Barkhausen phenomenon, that can be successfully used for pedagogical and simulation purposes.

VII. ACKNOWLEDGMENTS

The work of K. Kovács was supported by the KPI Sapientia Foundation. Z. Néda acknowledges a NATO research fellowship, the hospitality and stimulating atmosphere of the Centro de Fisica do Porto.

[1] J. P. Sethna, K. A. Dahmen, Ch. R. Myers, Nature, **410**, 242 (2001)
[2] G. Durin and S. Zapperi, cond-mat/0404512, 2004
[3] D. Spasojevic, S. Bukvic, S. Milosevic, H. E. Stanley, Phys. Rev. E **54**, 2531 (1996)
[4] P. Plewka, J.J. Zebrowski, M. Urbanski, Phys. Rev. E **57**, 6422 (1998)
[5] K. P. O'Brien, M. B. Weissman, Phys. Rev. E **50**, 3446 (1994)
[6] P. Bak, C. Tang, K. Weisenfeld, Phys. Rev. Lett. **59**, 381 (1987)
[7] K. L. Babcock, R. M. Westervelt, Phys. Rev. Lett. **64**, 2169 (1990)
[8] P. Bak, H. Flyvbjerg, Phys. Rev. A **45**, 2192 (1992)
[9] P. J. Cote, L. V. Meisel, Phys. Rev. Lett. **67**, 1334 (1991), Phys Rev. B **46**, 10822 (1992)
[10] B. Alessandro, C. Beatrice, G. Berotti, A. Montorsi, J. Appl. Phys. **68**. 2901, 2908 (1990)
[11] A. Travesset, R. A. White, K. A. Dahmen, Phys. Rev. B **66**, 024430 (2002)
[12] O. Perkovic, K. Dahmen, J.P. Sethna, Phys. Rev. Lett. **75**, 4528 (1995)
[13] O. Narayan, Phys. Rev. Lett. **77**, 3855 (1996)

[14] J. Urbach, R. Madison, J. Markert, Phys. Rev. Lett. **75**, 276 (1995)
[15] J. Mnyukh, Fundamentals of Solid-State Phase Transitions, Ferromagnetism and Ferroelectricity (Autorhouse, 2001)
[16] G. Durin, P. Cizeau, S. Zapperi, H.E. Stanley, J. Phys. IV France **8**, Pr2-319 (1998)
[17] M. Bahiana, B. Koiller, S. L. A. de Queiroz, J. C. Denardin, R. L. Sommer, Phys. Rev. E **59**, 3884 (1999)
[18] R.A. White and K.A. Dahmen, Phys. Rev. Lett. **91**, 085702 (2003)